BEAM STABILITY EXPERIMENTS ON DARHT-II

Carl Ekdahl, P. Aragon, E. O. Abeyta, R. Bartsch, L. Caudill, K. C. D. Chan, D. Dalmas, S. Eversole, R. Gallegos, J. Harrison, J. Johnson, E. Jacquez, B. Trent McCuistian, N. Montoya, S. Nath, K. Nielsen, D. Oro, L. Rodriguez, P. Rodriguez, L. Rowton, M. Sanchez, R. Scarpetti, M. Schauer, D. Simmons, H. V. Smith, J. Studebaker, G. Sullivan, and R. Temple,
Los Alamos National Laboratory, Los Alamos, NM 87545, USA
H. Bender, W. Broste, C. Carlson, G. Durtschi, D. Frayer, D. Johnson, K. Jones, A. Meidinger, K. Moy, R. Sturgess, A. Tipton, and C. Y. Tom, *Bechtel Nevada, Los Alamos, NM 87544, USA*
M. Schulze, *General Atomics, San Diego, CA 92121, USA*
T. Hughes, C. Mostrom, and Y. Tang, *ATK-Mission Research, Albuquerque, NM 87110, USA*
R. Briggs, *SAIC, Walnut Creek, CA 94596, USA*

Abstract

When completed, the DARHT-II linear induction accelerator (LIA) will produce a 2-kA, 18-MeV electron beam with more than 1500-ns current/energy "flat-top." In initial tests DARHT-II has already accelerated beams with current pulse lengths from 500-ns to 1200-ns full-width at half maximum (FWHM) with more than1.2-kA, 12.5-MeV peak current and energy. New experiments are planned with a ~1600-ns pulse length, but with reduced current and energy. These pulse lengths are all significantly longer than any other multi-MeV LIA, and they define a novel regime for high-current beam dynamics, especially with regard to beam stability. Although the initial tests demonstrated absence of BBU, the pulse length was too short to determine whether ion-hose instability would be present toward the end of a pulse longer than 1500-ns. The 1600-ns pulse experiments are designed to resolve these and other beam-dynamics issues with a long-pulse beam.

I. INTRODUCTION

Commissioning of DARHT-II is proceeding in three phases. The first phase was a demonstration that the DARHT-II technology could produce and accelerate a beam of electrons [1,2]. The second phase includes a demonstration of beam stability for the full pulse length of the final configuration. The major beam dynamics concerns for the accelerator are corkscrew motion, the beam breakup instability (BBU), and the ion-hose instability. To satisfy the requirements for DARHT-II, the rms beam motion at the accelerator exit due to all of these causes must be less than 10% of the beam radius (e.g., less than ~500 to 700 microns).

The long-pulse stability tests are now underway. To date we have produced and accelerated beams with a ~1600-ns "flat-top" current pulse, which are much longer than the pulses of the initial experiments [2]. The parameters of the accelerator and beam are shown in Table 1 for the initial experiments performed in 2002-2003 (Configuration "A"), the present beam stability test (Configuration "B"), and the final DARHT-II configuration, which will first be tested in 2007. Because the parameters of the final configuration are different than the parameters for the present experiments, we validated the stability of the final configuration by scaling our present experiments to have the same amplification as the final configuration would.

For example, the gain of the BBU is proportional to the number of cells and the beam current, and is inversely proportional to the strength of the magnetic guide field. Since the current and number of cells are both less in the present experiments than in the final configuration, we had to reduce the guide field strength until the BBU gain was that which would be expected for the final configuration.

Table 1. DARHT-II Parameters

Configuration:	**A**	**B**	**Final**
Beam Current (kA)	1.2-1.3	1.3	2.0
Pulse Length (μs)	0.5-1.2 FWHM	1.6 μs Flat	1.5 Flat
Diode Voltage (MV)	3.0	2.5	3.2
Injector Cells	8	6	6
Injector Cells (MeV)	1.2	0.54	1.1
Injector Energy (MeV)	4.2	3.04	4.3
Installed Accelerator Cells	64	50	68
Accelerator length (m)	36	28	43
Active Accelerator Cells	61-62	42	68
Exit Energy (MeV)	12.5	6.7	17

Likewise, the ion-hose gain is proportional to the length of the accelerator, the current, and the background gas pressure. Therefore, we scaled our shorter, lower-current experiments by increasing the background gas pressure

Report Documentation Page

Form Approved
OMB No. 0704-0188

1. REPORT DATE	2. REPORT TYPE	3. DATES COVERED
JUN 2005	**N/A**	**-**

4. TITLE AND SUBTITLE
Beam Stability Experiments On Darht-II

5a. CONTRACT NUMBER
5b. GRANT NUMBER
5c. PROGRAM ELEMENT NUMBER

6. AUTHOR(S)

5d. PROJECT NUMBER
5e. TASK NUMBER
5f. WORK UNIT NUMBER

7. PERFORMING ORGANIZATION NAME(S) AND ADDRESS(ES)
Los Alamos National Laboratory, Los Alamos, NM 87545, USA

8. PERFORMING ORGANIZATION REPORT NUMBER

9. SPONSORING/MONITORING AGENCY NAME(S) AND ADDRESS(ES)

10. SPONSOR/MONITOR’S ACRONYM(S)

11. SPONSOR/MONITOR’S REPORT NUMBER(S)

12. DISTRIBUTION/AVAILABILITY STATEMENT
Approved for public release, distribution unlimited

13. SUPPLEMENTARY NOTES
See also ADM002371. 2013 IEEE Pulsed Power Conference, Digest of Technical Papers 1976-2013, and Abstracts of the 2013 IEEE International Conference on Plasma Science. IEEE International Pulsed Power Conference (19th). Held in San Francisco, CA on 16-21 June 2013.

14. ABSTRACT
When completed, the DARHT-II linear induction accelerator (LIA) will produce a 2-kA, 18-MeV electron beam with more than 1500-ns current/energy flat-top. In initial tests DARHT-II has already accelerated beams with current pulse lengths from 500-ns to 1200-ns fullwidth at half maximum (FWHM) with more than1.2-kA, 12.5-MeV peak current and energy. New experiments are planned with a ~1600-ns pulse length, but with reduced current and energy. These pulse lengths are all significantly longer than any other multi-MeV LIA, and they define a novel regime for high-current beam dynamics, especially with regard to beam stability. Although the initial tests demonstrated absence of BBU, the pulse length was too short to determine whether ionhose instability would be present toward the end of a pulse longer than 1500-ns. The 1600-ns pulse experiments are designed to resolve these and other beam-dynamics issues with a long-pulse beam.

15. SUBJECT TERMS

16. SECURITY CLASSIFICATION OF:			17. LIMITATION OF ABSTRACT	18. NUMBER OF PAGES	19a. NAME OF RESPONSIBLE PERSON
a. REPORT	b. ABSTRACT	c. THIS PAGE			
unclassified	**unclassified**	**unclassified**	**SAR**	**6**	

until we had the ion-hose gain expected for the final configuration.

I. ACCELERATOR

The 88-stage Marx generator that powers the injector diode for DARHT-II is capable of producing a 3.2-MV output pulse that is flat for 2-μs, but we are operating it at 2.5 MV to provide a greater margin of protection for the insulating column.After leaving the diode, the beam is accelerated by large-bore (36-cm-diam beam tube) induction cells to 3.04 MeV. Originally, eight of these completed the injector in the initial experiments (configuration "A"), and six of these are now installed for the long-pulse stability experiments (configuration "B").

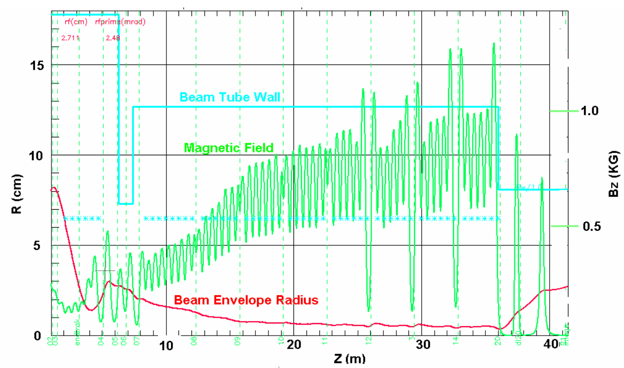

Figure 1. Scheme of DARHT-II for long-pulse stability experiments (configuration B). The beam envelope radius calculated by the XTR code is shown in red. The solid green line is the strength of the solenoidal magnet field on axis. The radius of the beam tube is shown by the solid cyan line. The cyan asterisks indicate the location and accelerating potentials of the cells (90 keV). The vertical green dashed lines indicate the locations of beam position monitors.

Following the injector, there is a special transport zone designed to scrape off the long rise time, off-energy beam head. As in the initial experiments [1,2], this beam-head clean-up zone (BCUZ) is presently configured to pass the entire beam head, and the timing of the induction cells is set to accelerate the ~500-ns risetime, off-energy beam head, as well as the flat top. The magnetic tune through the BCUZ compresses the beam to the smaller radius needed to match into the main accelerator.

The main accelerator consists of smaller-bore (25.4-cm-diam beam tube) "standard" induction cells for the long-pulse stability experiments. Several of these are presently inactive. The magnetic tune through the main accelerator gradually increases to a field of more than 1 kG on axis to suppress BBU. The tunes for these experiments were designed using the XTR envelope code [3]. For the initial experiments self-consistent initial conditions for XTR were established using the TRAK ray-tracing code [4, 5]. For the present experiments we are also using the LSP particle in cell code [6] to provide initial conditions.

DARHT-II is heavily instrumented with beam and pulsed-power diagnostics [2]. There are beam position monitors (BPMs) in the diode anode region, one at the exit of the injector cells, one in the BCUZ, one at the entrance to each block of six cells, one at the accelerator exit, and one just before the imaging target. The BPMs are based on arrays of azimuthal B-field detectors [7, 8], and also measure the beam current. Streak and framing cameras produce images of beam-generated Cerenkov and optical transition radiation (OTR) light from targets inserted in the beam line. Finally, a magnetic spectrometer is used to measure the beam-electron kinetic energy.

II. RESULTS AND DISCUSSION

The new cathode installed for the stability tests produces as much current at 2.5 MV diode voltage as the original cathode did at 3.0 MV. This is ~90% of the current predicted for our diode by both the TRAK ray-tracing gun-design code and the LSP PIC code. The injector cells then accelerated the beam without loss of current within the ~2% uncertainty of the measurement (Fig. 2 and Fig. 3).

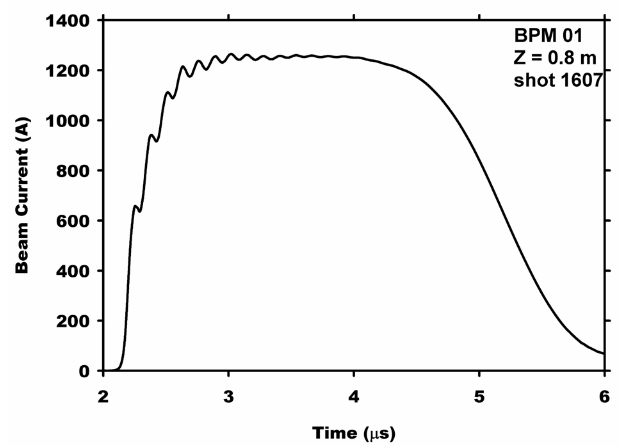

Figure 2. Beam current at exit of diode (entrance to injector cells) showing 7.8-MHz LC oscillations.

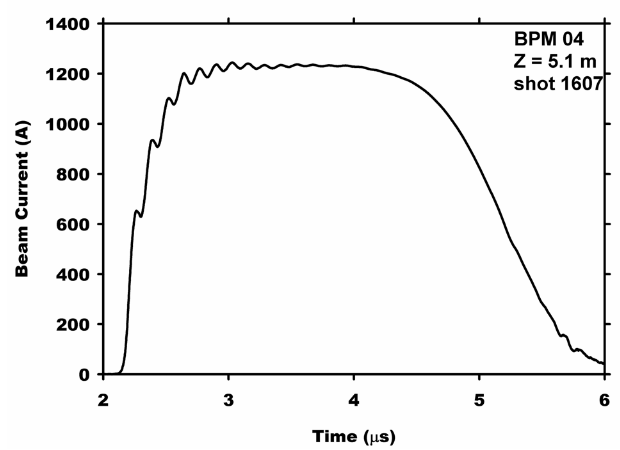

Figure 3. Beam current at exit of injector cells (entrance to BCUZ).

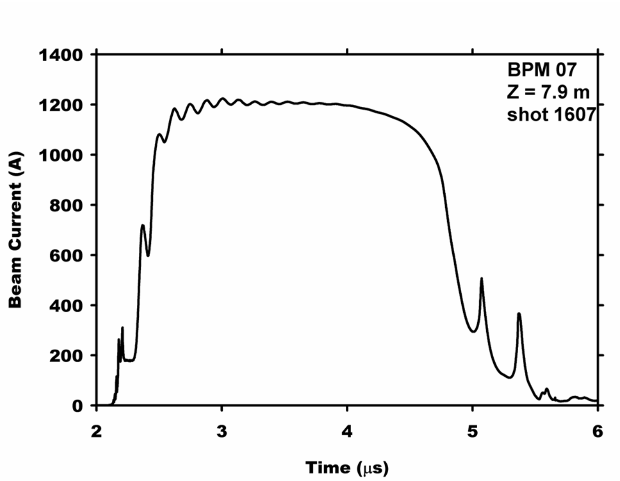

Figure 4. Beam current at entrance to accelerator (exit of BCUZ).

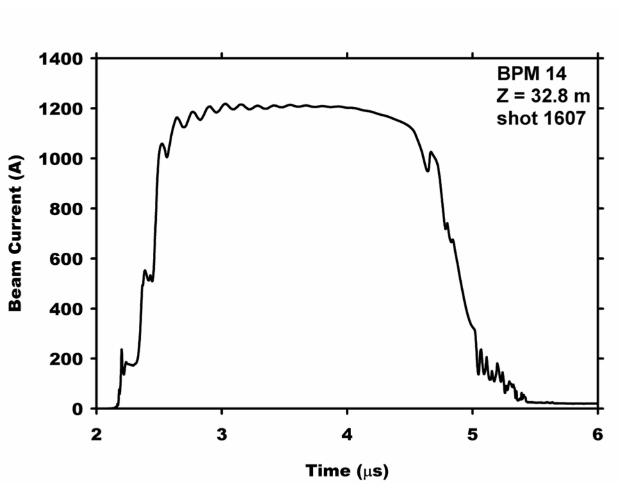

Figure 5. Beam current at last cell block of accelerator.

Some of the beam head and tail were scraped off in the BCUZ throat, and then very little further loss occurred as the beam was accelerated through the remaining accelerator cells (Fig. 4 and Fig. 5). There was no evidence of beam loss due to either BBU or ion-hose, and the beam motion at the end of the accelerator due to these instabilities was negligible throughout the entire pulse for this tune.

A. Corkscrew Motion

Corkscrew motion is a concern for accelerators such as DARHT that use solenoidal magnetic fields for transporting and focusing the beam [9,10]. This effect is caused by the interaction of energy variation during the beam pulse with random dipoles resulting from solenoid misalignments. The amplitude of this "random" corkscrew is predicted to grow through the accelerator in proportion to $N_s^{3/2}\delta\Theta_{rms}\delta\gamma/\gamma$, where N_s is the number of solenoids, $\delta\Theta_{rms}$ is the rms misalignment, and $\delta\gamma/\gamma$ is the electron energy variation [10].

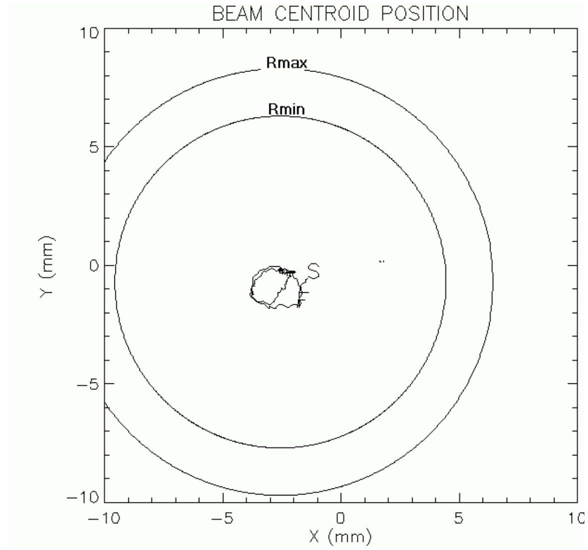

Figure 6. Beam position at accelerator exit during a 400-ns window around peak current compared with estimated beam size from XTR envelope code for a probable range of initial conditions. (S and F signify start and finish of trajectory).

In addition to the random corkscrew the DARHT-II accelerator has a large corkscrew generated in the diode. This is produced by the 7.8-MHz LC oscillation on the main voltage pulse, which is caused by the capacitances and inductances of the injector structure. The 7.8-MHz electron energy oscillation in the diode causes a small oscillation of the beam position through interaction with an accidental magnetic dipole in the diode region. This linear motion is modified into corkscrew [9] as the beam transports through the bumpy solenoid magnetic field. However, it is not amplified, and remains less than 20% of the beam radius at the exit of the accelerator (Fig 6). If one ignores the 7.8-MHz corkscrew in Fig. 6 it is obvious that the residual motion due to all other causes (including the aforementioned random corkscrew) is much less than 200 micron in amplitude.

One concern about corkscrew motion is the possibility that it could seed the BBU. Obviously, the 7.8 MHz corkscrew is not a problem in this respect. However, there is high frequency beam motion evident in data at the diode exit that is in the BBU frequency range. The 7.8-MHz oscillations are such a strong feature of the beam motion that they completely dominate any frequency analysis. Therefore, we filtered them out using a narrow, 2-MHz wide, notch filter. The result of the filtered frequency analysis of dy/dt is shown in Fig. 7. (We analyzed velocity measurements because they are more sensitive to high frequency motion than position measurements by a factor of ω.) It is clear that there is substantial beam motion in the frequency range of the lowest BBU mode, with pronounced motion at 100 MHz. Presumably this is due to a 100-MHz RF mode predicted in early simulations of the injector vacuum vessel. Even through the measured rms amplitudes of these high-frequency corkscrew modes are only ~ 100 micron or less, they could effectively seed the BBU in the accelerator.

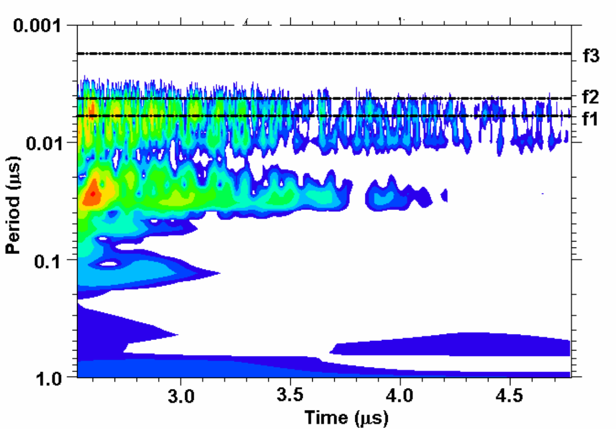

Figure 7. Frequency analysis of dy/dt during 2-ms flat top of current pulse. (The 7.8 MHz oscillations were filtered out for this analysis.)

B. Beam Breakup

During the initial experiments on DARHT-II we tested the accelerator for its immunity to the BBU instability [11]. BBU frequencies for the accelerator cells are 169 MHz, 236 MHz, and 572 MHz [12]. In an infinitely long pulse, the maximum amplification from the BBU is expected to be $(\gamma_0/\gamma)^{1/2}\exp(\Gamma_m)$ throughout the length of the accelerator, where $\Gamma_m = I_b N_g Z_\perp \langle 1/B \rangle / 3\text{x}10^4$ [11-14]. Here, I_b is the beam current in kA, the transverse impedance $Z_\perp$ is in Ω/m, and the $\langle 1/B \rangle$ is in kG^{-1} (the brackets < > denote average over accelerator length). A sinusoidal excitation at the resonant frequency is predicted to grow to this maximum amplification and then saturate due to resistive energy losses in the cells.

In DARHT-II the BBU grows rapidly out of seed motion such as the high-frequency corkscrew or random noise on the beam, since there is no sharp risetime to excite it. (As shown in Fig. 7 there is ample motion excited in the diode to seed the BBU.) The time to grow to maximum is $\tau_m = 2\Gamma_m Q/\omega_0$, which is less than 25 ns for all BBU modes of DARHT-II. (Here, Q is the cavity quality factor and ω_0 is the mode resonant frequency.) Because this time to saturation is so short, we would have discovered any problems with BBU in the initial, 500 to 1200-ns FWHM "short-pulse" experiments. No evidence of BBU growth was seen in those initial experiments until the magnetic field strength was reduced 1/5 the value of the nominal tune throughout the accelerator, at which point amplification at the lowest frequency BBU mode was observed [1, 2].

We repeated these tests with our 1600-ns flat-top pulse, retuning the magnetic guide field until we had a BBU gain approximately equal to that expected for the final accelerator configuration. For a representative shot using that tune, Figure 8 shows the beam motion at the entrance of the accelerator, and Figure 9 shows the motion at the accelerator exit, where the amplitude is less than 200 microns. We quantified the BBU gain by integrating the power spectrum over the entire 150 to 200-MHz band and comparing the output to the input, which gives an integrated amplitude amplification of 1.75, compared with a predicted amplification of 1.8.

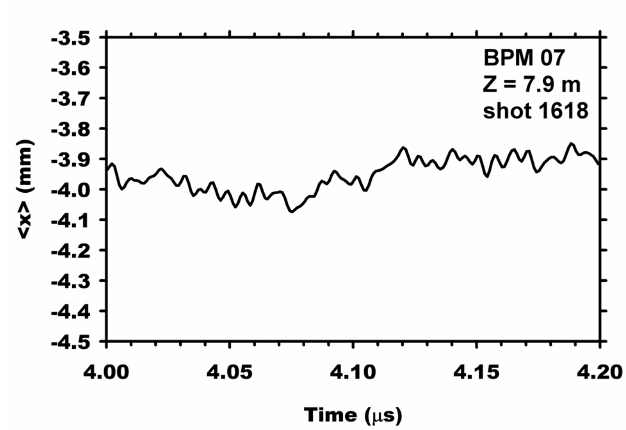

Figure 8. Beam motion in the horizontal plane at the entrance to the accelerator during a 200-ns window near the end of the current flat top. The tune used for this shot was scaled to give the same gain as for the final configuration.

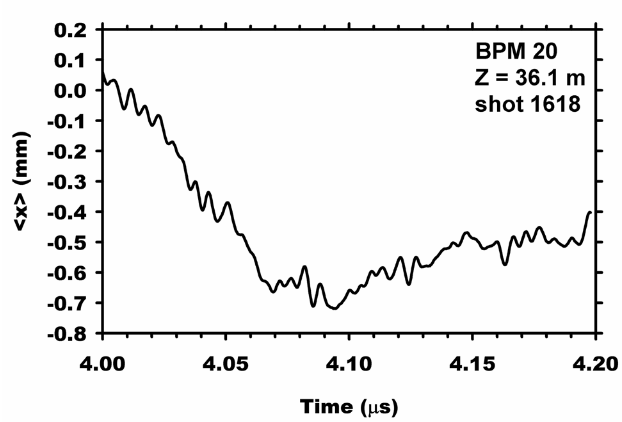

Figure 9. Beam motion in the horizontal plane at the exit of the accelerator during a 200-ns window near the end of the current flat top. The tune used for this shot was scaled to give the same gain as for the final configuration.

By further reducing the magnetic field to increase the predicted Γ_m by 50% we were able to increase this integrated amplification to 3.6, which still resulted in less than 500 micron amplitude at the end of the accelerator. Figure 10 shows the beam motion at the exit of the accelerator for this tune.

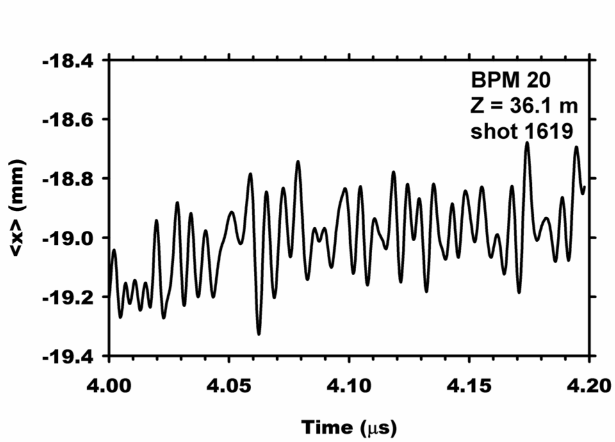

Figure 10. Beam motion in the horizontal plane at the exit of the accelerator during a 200-ns window near the end of the current flat top. The tune used for this shot was scaled to give 50% greater gain than the final configuration.

C. Ion Hose Instability

Because of the long pulse of DARHT-II the ion-hose instability [16] is of some concern, and a substantial effort has been paid to the accelerator vacuum. In a strong axial guide field such in DARHT-II, the amplification of the ion hose in N_2 background gas is $\exp(\Gamma)$, where $\Gamma \simeq 6\times10^{-2} I_b \left\langle p/\left(B_z a^2\right)\right\rangle \tau L$ for a pulse length τ (μs) at the end of L (m) [17]. Here, the background pressure p is in μTorr, the beam radius a is in cm, the guide field B_z is in kG, the beam current I_b is in kA, and the brackets denote the average over length. For the DARHT-II final configuration, $\Gamma \sim 1$ for a pressure of about 0.2 μTorr, so the vacuum system is interlocked to prevent accelerator operation if the pressure exceeds 0.1 μTorr. The normal base pressure is less than half the interlock pressure, as shown in Fig. 11.

To replicate the ion-hose growth that would be expected in the final configuration, we increased the base pressure by valving off all of the accelerator vacuum pumps, and then bleeding air into the system. This resulted in the profiles with maxima greater than 10^{-7} Torr shown in Fig. 11. The scaling factor from our configuration (B) to the final configuration is (43m/28m)x(2.0 kA/1.25 kA) = 2.46. Therefore, the profile with maximum pressure ~4.6×10^{-7} Torr would produce ion hose growth in the final configuration with a maximum pressure of ~1.9×10^{-7} Torr, or about twice the normal interlock setting.

Figure 12 shows the beam motion at the entrance to the last cell block during a 400-ns window near the end of the current flat top for the shot with this profile. The ion-hose frequency for N_2 is $f = 10/a$ MHz, where the beam radius a is in cm [17]. For the DARHT-II tunes, this gives frequencies between 10 and 20 MHz.. We filtered out the residual 7.8-MHz corkscrew with a notch filter to clarify the ion-hose motion in this frequency range, which is barely discernable for this pressure profile (Fig. 12).

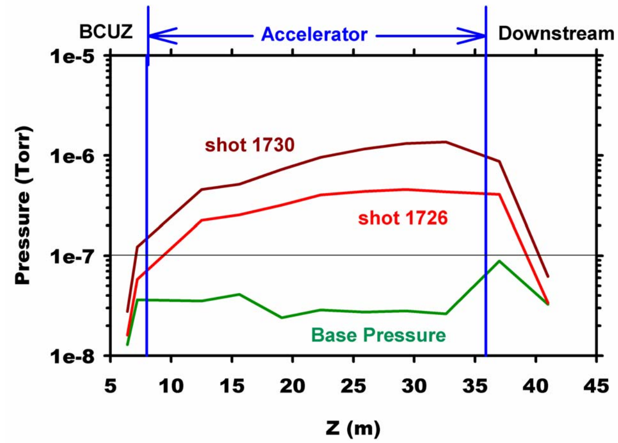

Figure 11. Pressure profiles used in the ion-hose tests. The accelerator is normally interlocked so that it cannot operate if the pressure exceeds 10-7 Torr.

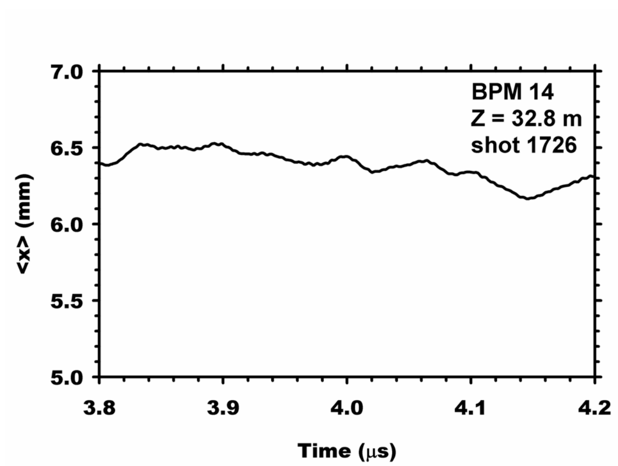

Figure 12. Beam motion at the entrance to the last cell block for a pressure profile corresponding to a maximum pressure of ~ 1.9 x 10^{-7} Torr for the final configuration. (The 7.8-MHz corkscrew has been filtered out of these data to clarify motion in the 10 to 20-MHz frequency range characteristic of ion-hose.)

To accentuate the ion hose motion, we further increased the pressure to the equivalent of 6 x 10-7 Torr in the final configuration. Fig. 13 shows the beam motion at the entrance to the last cell block during the same 400-ns window near the end of the current flat top. The presence of the ion-hose is quite evident in these data, which also have the 7.8-MHz corkscrew filtered out.

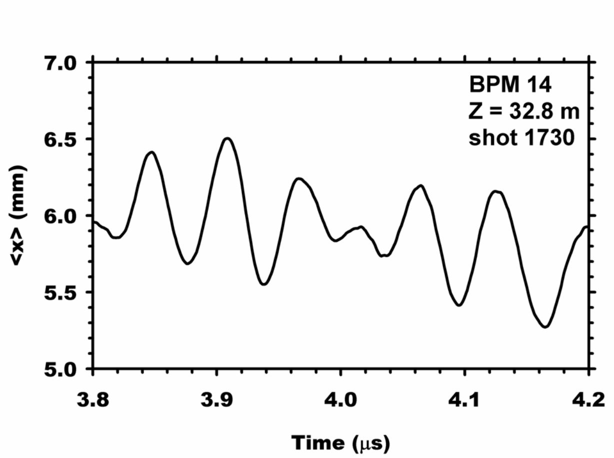

Figure 13. Beam motion at the entrance to the last cell block clearly showing the ion-hose motion when the maximum pressure was increased to the equivalent of 6 x 10^{-7} Torr in the final configuration. (The 7.8-MHz corkscrew has been filtered out of these data to clarify motion in the 10 to 20-MHz frequency range characteristic of ion-hose.)

III. CONCLUSIONS

The DARHT-II beam pulse has a large amplitude corkscrew at 7.8 MHz excited by LC oscillations in the diode. In addition, there are high frequency, small amplitude corkscrew gyrations which may seed the BBU, even though they are less than 200-micron amplitude in the accelerator.

However, all experiments to date show that the maximum BBU growth in the accelerator is acceptably small with the nominal tunes used. (N. B. The maximum magnetic field that can be applied in the final configuration would further reduce Γ_m by another 30% below that attained with the final tunes on which we based our scaling.) Moreover, we have yet to observe the higher frequency BBU modes in our present experiments, in which we have adequate system bandwidth for the measurement.

The amplitude of the ion-hose instability was less than 200 microns even when we increased the background pressure to a value equivalent to twice the final accelerator interlock pressure. By increasing the background gas pressure further we were able to clearly observe the ion hose instability in the predicted frequency range.

Based on these scaled experiments, we expect that the motion due to all of these effects will be less than 10% of the beam radius at the accelerator exit; well within the performance requirements for DARHT-II.

IV. ACKNOWLEDGEMENTS

This work was supported by the US National Nuclear Security Agency and the US Department of Energy under contract W-7405-ENG-36.

V. REFERENCES

[1] Carl Ekdahl, et al., "First beam at DARHT-II," in Proc. 2003 Part. Accel. Conf., 2003, pp. 558-562

[2] Carl Ekdahl, et al., "Initial electron-beam results from the DARHT-II linear induction accelerator," IEEE Trans. Plasma Sci., vol. 33, pp. 892-900, April 2005

[3] Thomas P. Hughes, David C. Moir and Paul W. Allison, "Beam injector and transport calculations for ITS," in Proc. 1995 Part. Accel. Conf., 1995, pp. 1207-1209

[4] Carl Ekdahl, "Beamline tunes for DARHT-II phase-1 commissioning," Los Alamos National Laboratory report LAUR-02-3921, June 27, 2002

[5] Stanley Humphries Jr., "TRAK – Charged particle tracking in electric and magnetic fields," in Computational Accelerator Physics, R. Ryne Ed., New York: American Institute of Physics, 1994, pp. 597-601

[6] T. P. Hughes, R. E. Clark, and S. S. Yu, "Three-dimensional calculations for a 4 kA, 3.5 MV, 2 microsecond injector with asymmetric power feed," Phys. Rev. ST Accel. Beams, vol. 2, 110401, 1999

[7] C. A. Ekdahl, "Fourier-analyzing coil arrays for pulsed relativistic electron beam experiments," Rev. Sci. Instrum., vol. 55, 1984, pp. 1221-1228

[8] Carl Ekdahl, "Aliasing errors in measurements of beam position and ellipticity," accepted by Rev. Sci. Instrum., 2005

[9] G. J. Caporaso, et al., "Beam dynamics in the Advanced Test Accelerator (ATA)," in Proc. 5th Int. Conf. on High-Power Particle Beams, pp. 427-432, 1983

[10] Yu-Jiuan Chen, "Corkscrew modes in linear accelerators," Nuc. Instrum. Meas., vol. A292, pp. 455-464, 1990

[11] V. K. Neil, L. S. Hall, and R. K. Cooper, "Further theoretical studies of the beam breakup instability," Particle Accelerators, vol. 9, pp. 213-222, 1979

[12] Y. J. Chen and W. M. Fawley, "BBU and Corkscrew Growth Predictions for the DARHT Second Axis Accelerator," in Proc. 2001 Part. Accel. Conf., 2001, pp. 3490-3492, 2001

[13] Carl Ekdahl, "Maximum amplitude of BBU growth in DARHT-II experiments," Los Alamos National Laboratory Report LAUR-04-3915, June, 2004

[14] G. J. Caporaso, "The control of beam dynamics in high energy induction linacs," in Proc.1986 Linear Accel. Conf., 1986, p. 17

[15] A. W. Chao, B. Richter, and C-Y Yao, "Beam emittance growth caused by transverse deflecting fields in a linear accelerator," Nucl. Instrum. Methods, vol. 178, pp. 1-8, 1980

[16] H. L. Buchanan, "Electron beam propagation in the ion-focused regime," Phy. Fluids, vol. 30, pp. 221-231, 1987

[17] R. Briggs, "Transverse instabilities from ion oscillations in the DARHT-II accelerator," LBNL Engineering Note M7848, January, 2000